Food Quality and Safety, 2023, **7**, 1–13
https://doi.org/10.1093/fqsafe/fyad030
Advance access publication 21 August 2023
Article

OXFORD

Article

Preparation and characterization of octenyl succinic anhydride nano starch from tiger nut meals

Jian Wang (王舰)[1,†,*], Rui Zhang (张瑞)[1,†], Zhenyu Huang (黄镇宇)[1], Ming Cai (蔡铭)[1], Wenyu Lou (楼文雨)[1], Yan Wang (王龑)[1], Adem Gharsallaoui[2], Hynek Roubik[3], Kai Yang (杨开)[1,*], and Peilong Sun (孙培龙)[1,*]

[1]College of Food Science and Engineering, Key Laboratory of Food Macromolecular Resources Processing Technology Research, Zhejiang University of Technology, Hangzhou, China
[2]CNRS, LAGEPP UMR 5007, Univ. Lyon, Université Claude Bernard Lyon 1, Villeurbanne, Lyon, France
[3]Department of Sustainable Technologies, Faculty of Tropical AgriSciences, Czech University of Life Sciences Prague, Prague, Czech Republic

[†]These authors contributed equally to this work.
[*]*Correspondence to*: Jian Wang, College of Food Science and Engineering, Key Laboratory of Food Macromolecular Resources Processing Technology Research, Zhejiang University of Technology, No. 18, Chaowang Road, Hangzhou 310014, China. E-mail: Wangjian1926@zjut.edu.cn, wangjian1926@gmail.com; Kai Yang, College of Food Science and Engineering, Key Laboratory of Food Macromolecular Resources Processing Technology Research, Zhejiang University of Technology, No. 18, Chaowang Road, Hangzhou 310014, China. E-mail: Yangkai@zjut.edu.cn; Peilong Sun, College of Food Science and Engineering, Key Laboratory of Food Macromolecular Resources Processing Technology Research, Zhejiang University of Technology, No. 18, Chaowang Road, Hangzhou 310014, China. E-mail: Sun_pl@zjut.edu.cn

Abstract

Tiger nut (*Cyperus esculentus* L.) is an ideal raw material for oil extraction, but starch-rich tiger nut meal, a by-product of oil extraction, has not been fully utilized. For this, starch was isolated from tiger nut meal, and then starch nanoparticles were prepared by gelatinization, ultrasonication and nanoprecipitation under different conditions. The preparation parameters were optimized by measuring the particle size with dynamic light scattering, and the physicochemical properties of native starch and nano starch were evaluated. The results showed that, compared to native starch, starch nanoparticle (nano starch) has a higher amylose content (39.05%), solubility (56.13%), and swelling power (58.01%). Furthermore, native starch and nano starch were esterified with octenyl succinic anhydride (OSA), respectively, conferring amphiphilic properties. The effects of OSA modification on the resistant starch content, thermal properties, and microstructure of starches were characterized. The resistant starch content of tiger nut native starch increased by 10.81% after OSA modification, while the resistant starch content of OSA nano starch increased to 37.76%. Compared to native starch, the gelatinization temperature of OSA nano starch decreased by 2.7 °C and nano starch decreased by 5.68 °C. OSA modified nano starch showed a unique microstructure, such as a slender fiber structure and a regular oblate structure. The hydrophobic OSA groups aggregated to form hydrophobic cavities with a hydrophilic surface in the aqueous phase. The findings presented in this investigation provide a better understanding of the design and development of OSA nano starch and provide valuable guidance to further enhance the added value of tiger nuts and future applications in the food industry.

Keywords: tiger nut starch; ultrasonication; nanoprecipitation; modification; OSA nano starch; physicochemical properties.

Introduction

Tiger nut, as the tuber of *Cyperus esculentus* L., is an ideal natural crop that originated in Egypt and dates back to the fifth millennium BC (Defelice, 2002). In the Middle Ages, the Arab civilization brought tiger nuts to Spain, where they were processed into a kind of refresh beverage named 'horchata de chufa' from the thirteenth century (Pascual *et al.*, 2000; Cortés *et al.*, 2005). Today, the popularity of tiger nuts has been extended from Mediterranean regions to Europe, Africa, America, China, and other areas with various applications (Sánchez-Zapata *et al.*, 2012). Among these, tiger nut is considered to be an ideal raw material for oil extraction, due to its high quantity and quality (with a similar lipid profile to olive oil) of lipids (Ezeh *et al.*, 2014). After squeezing the oil, tiger nut meal as a co-product is usually applied to feed animals, which could lead to a large waste of resources. Therefore, the isolation of starch from tiger nut meals has received increasing attention for the total utilization of tiger nut, because of its high content (26%–42%, dry weight) in tiger nut (Liu *et al.*, 2019, 2020). Furthermore, the modification of tiger nut starch has also been gradually attracting the attention of researchers to improve its industrial implications (Li *et al.*, 2017; Yan *et al.*, 2022).

Among the various methods of starch modification, the synthesis of starch-based nanoparticles, which have a dimension smaller than 200 nm (Sun, 2018), has attracted extensive attention. Due to their small dimension, the surface–volume ratio is high, and starch nanoparticles display specific characteristics that make them superior to native starch, such as less light scattering, higher stability, higher solvability, and higher permeability to bio-barriers (Yu *et al.*, 2021). Meanwhile,

Received 4 May 2023; Revised 20 June 2023; Editorial decision 7 July 2023

nano starch inherits the excellent characteristics of native starch, such as biocompatibility, biodegradability, and sustainability, which have potential applications in food, drug delivery carriers, and biodegradable edible films. Meanwhile, starch can be modified by octenyl succinic anhydride (OSA) to give it an adjustable amphiphilic property (Altuna *et al.*, 2018). Due to a combination of the hydrophobic property of OSA and the high-branched structure unique to starch, OSA-modified starch possesses remarkable interfacial, stabilizing, rheological, encapsulating, and nutritional properties, which make OSA starch widely utilized in the food industry for over a half century as emulsifiers, embedding agents, fat substitutes, and slowly digestible starches (Sweedman *et al.*, 2013; Zhang *et al.*, 2021). Recently, the combination of nanotechnology and OSA modification has been applied to quinoa, maize, and potato starches (Ye *et al.*, 2017a; Li and Gao, 2023; Remanan and Zhu, 2023). However, to our knowledge, few studies have reported on the preparation of OSA nano starch from tiger nut.

In this study, tiger nut starch was first isolated, and then starch nanoparticles were synthesized by gelatinization, ultrasonication, and nanoprecipitation under different conditions. After optimization of nano starch preparation by measuring particle size, the physicochemical properties of native starch and nano starch were compared. Furthermore, OSA modification was applied to both native starch and nano starch, conferring amphiphilic properties. The intention of this research is to study the effects of OSA modification and nanoprecipitation treatment on the physicochemical properties and microstructure of starch from tiger nut meals. The outcome of this investigation may provide a better understanding of the design and manufacturing of OSA nano starch, and provide valuable guidance to improve the added value of tiger nuts and future applications in the food industry.

Materials and Methods

Materials

Tiger nut (*Cyperus esculentus* L.) meal was obtained from tiger nut products after oil pressing from Jilin Fuxiang Biotechnology Company (Changchun, China). Absolute ethanol (99.7%) was purchased from Fangping Chemical Co., Ltd. (Hangzhou, China). Octenyl succinic anhydride (OSA) was obtained from Bide Pharmatech., Ltd. (Shanghai, China). Alpha-amylase and maleic acid were purchased from Yuanye Bio-Technology Co., Ltd. (Shanghai, China). Amyloglucosidase (AMG) and glucose oxidase/peroxidase (GOPOD) reagents were purchased from Marklin (Shanghai, China). Acetic acid, ethanol, isopropanol, sodium hydroxide (NaOH), potassium hydroxide (KOH), and all other chemical reagents (Xilong Chemical Co., Ltd., Guangzhou, China) were of analytical grade.

Isolation of tiger nut starch

Tiger nut starch was isolated according to the Liu method with some modifications (Liu *et al.*, 2019). Briefly, tiger nut meal was de-oiled with petroleum ether at a ratio of 1:3 (mass concentration) at 25 °C for 24 h, washed with petroleum ether three times, and dried at 25 °C. The de-oiled tiger nut meal was added to 0.01 mmol/L sodium hydroxide solution at a proportion of 1:5 (mass concentration), stirred at ambient temperature for 6 h, and then centrifuged at 3000×*g* for 20 min (CR21N, Hitachi, Ltd., Tokyo, Japan). The centrifugal sediment was rinsed with water to neutral pH. To remove low-molecular-weight compounds, the starch residue was washed with 70% ethanol three times. The resulting starch fraction was thoroughly washed with deionized water, and then dried at 35 °C for 24 h to obtain native starch. The basic composition of the isolated tiger nut starch was as follows: the contents of starch, crude protein, fat, ash, and moisture were 70.18%, 0.31%, 0.23%, 2.15%, and 10.43%, respectively, and thefiber content was more than 10%.

Preparation of tiger nut starch nanoparticles

Tiger nut starch nanoparticles were prepared through gelatinization, ultrasonication, and nanoprecipitation, as shown in Figure 1, according to the methodology in previous publications (Ahmad *et al.*, 2020; Wang *et al.*, 2022). Briefly, a certain amount of tiger nut starch was added to deionized water to prepare the starch slurry, and then heated at 95 °C for 30 min for gelatinization. After gelatinization, the starch paste was treated ultrasonically for 10–30 min at ambient temperature using an ultrasonic instrument (JY98-IIIDN, Ningbo Scientz Biotechnology Co., Ltd., Ningbo, China) equipped with a 6-mm conical probe. To minimize heat generation, the output power was set as 600 W, and the on/off pulse was set as 3/5 s. After ultrasonication, the starch suspension solutions were diluted to certain concentrations (1%, 2%, 3%, 4%, and 5% (mass concentration)), and then rapidly poured into anhydrous ethanol (95%) under constant stirring. The volume ratios of starch slurry to anhydrous ethanol were 1:1, 1:2, 1:3, 1:4, and 1:5 . After nanoprecipitation, the starch solution was centrifuged (15 min, 4000×*g*), the supernatant was discarded, and the nano starch was obtained by freeze-drying (Scientz-12N, Ningbo Scientz Biotechnology Co., Ltd., Ningbo, China). The freeze-drying conditions were as follows: sample temperature was –40.4 °C, cold trap temperature was –57.9 °C, degree of vacuum was 4.8 Pa, and vacuum pump start cold trap temperature was –33 °C. Before freeze-drying, samples need to be frozen at –80 °C for 24 h in the refrigerator.

Particle size measurement

Dynamic light scattering technology (Zetasizer Nano ZS-90, Malvern Instruments Ltd., Malvern, UK) was applied to detect the average size and size distribution of starch nanoparticles. For the freeze-dried nano starch, the sample was first redispersed in deionized water to a mass fraction of 0.5%, and then ultrasonically treated in an ultrasound bath (SB-300DTY, Ningbo Scientz Biotechnology Co. Ltd., Ningbo, China) for 20 min to obtain a more uniform sample solution. Approximately 1 mL of sample solution was taken into a 1-cm glass cuvette for measurements. The refractive indices of water and starch were set as 1.33 and 1.53, respectively. Every sample was automatically detected five times by the instrument, and the average size (Z-average) and polydispersity index (PDI) of the starch nanoparticles were obtained.

Swelling power and solubility of native starch and nano starch

The determination of the solubility and swelling power of native starch and nano starch refers to Simsek's method with slight modification (Simsek *et al.*, 2012). A 0.2-g starch sample was placed in a 50-mL centrifuge tube filled with 20 mL distilled water to prepare the starch suspension. The

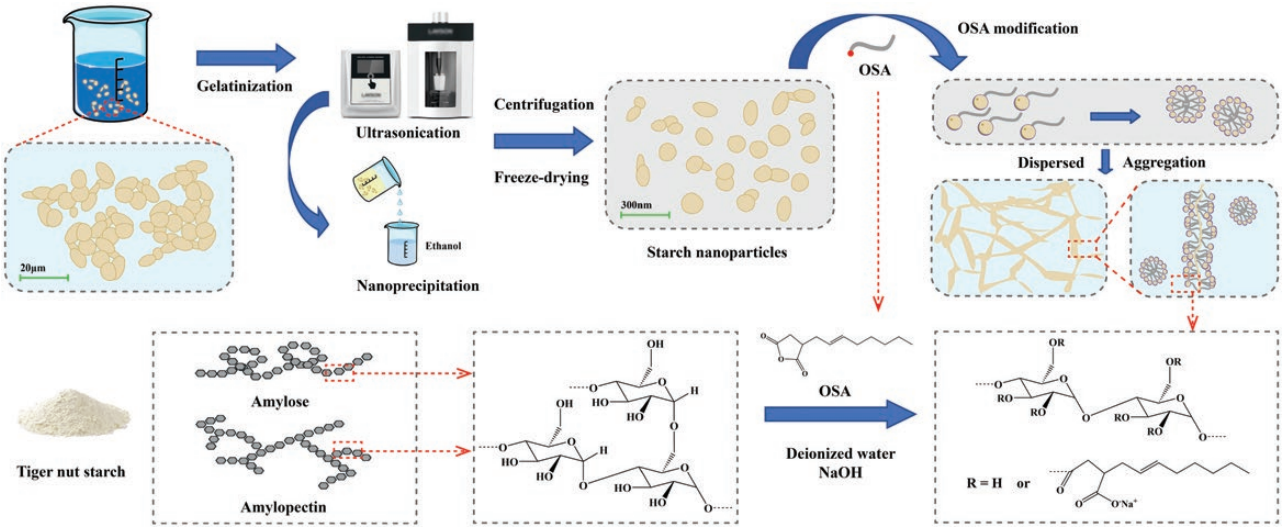

Figure 1. Preparation process of nano starch and mechanism diagram of octenyl succinic anhydride (OSA)-modified nano starch.

prepared starch suspensions were heated in a water bath at 55, 65, 75, 85, and 95 °C for 30 min, and shaken once every 5 min. After the heat treatment, the samples were cooled, centrifugally separated (3000×*g*, 4 °C, 15 min), and precipitated from the supernatant. The supernatant was poured into an aluminum dish and dried to a constant weight at 110 °C. The solubility and swelling of the starch samples were calculated according to the formulae:

$$S = A/W \times \ 100\%$$

$$P = B/[W \times (100\% - S)]$$

In the formulae, S is solubility (%), P is swelling (g/g), A is the constant weight of supernatant (g), W is the mass of the total sample (g), and B is the wet weight of precipitates (g).

OSA modification of tiger nut starch

Tiger nut native starch and nano starch were modified by OSA according to the method described by Ye *et al.* (2017b). Briefly, native starch or nano starch was dispersed in distilled water with consecutive stirring to obtain a starch slurry with a mass concentration of 35%. The pH of the starch slurry was adjusted to 8.5 with dilute alkali solution. Then, OSA (3%, on the basis of tiger nut starch weight; diluted three times with isopropanol) was slowly dropped into the starch slurry. The mixture was constantly stirred for the reaction, and the pH was kept at 8.5 with NaOH (Figure 1). After reaction for 2 h, the starch slurry was neutralized with 1 mol/L HCl to pH 6.0 to stop the reaction and then centrifuged at 3000×*g* for 15 min. The precipitates were washed twice with distilled water and three times with 70% ethanol solution, and then dried at 45 °C for over 24 h. OSA starch and OSA nano starch were obtained.

Resistant starch contents

The content of resistant starch in the tiger nut starch was determined by an enzymatic method (Khawas and Deka, 2016). After α-pancreatic amylase was added to the starch sample, it was incubated at 37 °C for 16 h. With passing time, the α-pancreatic amylase would hydrolyze the non-resistant starch in the samples into glucose. Then, an equal volume of ethanol solution was added to stop the reaction and resistant starch granules were obtained by centrifugation. The resistant starch was dissolved in 2 mol/L KOH and stirred at 4 °C for 20 min. These starch solutions were neutralized with sodium acetate buffer (pH 3.8) and the starch samples were hydrolyzed to glucose with AMG. Glucose was quantified by GOPOD to determine the resistant starch content in the sample.

Fourier transform infrared spectroscopy

The tiger nut starches were scanned by Fourier transform infrared spectroscopy (FT-IR; Nicolet iS50 iN10, Thermo Fisher Scientific, Waltham, MA, USA), with potassium bromide powder as the blank scanning background. Briefly, a sample was prepared by grinding tiger nut starches (1–2 mg) with potassium bromide powder (198 mg) and pressing it on a disk at 85 kPa for 5 min onto a disk. The spectra were scanned at 25 °C in a range from 4000 to 500 cm^{-1}.

X-ray diffraction

An X-ray diffractometer (Empyrean, PANalytical, Inc., Almelo, The Netherlands) was applied to determine the crystalline structures of starches. All starch samples were stored in an airtight container with a relative humidity of 85% for 24 h to obtain a constant moisture content before measurement. X-ray diffraction (XRD) patterns were measured at 25 °C. The X-ray diffraction patterns of starches were recorded using Cu–K_α radiation (λ=0.1541 nm). The working voltage and current were 45 kV and 40 mA, respectively. The patterns were recorded from 10° to 60° with a 2θ range at a step of 0.02°. MDI Jade 6.5 software was used to fit the XRD data (Material Data, Inc., Livermore, CA, USA), and a smooth curve was fitted under the diffraction peak. The crystallinity of starch depends on the crystalline peak diffraction area and the amorphous diffraction area.

Differential scanning colorimetry

The Perkin–Elmer Differential Scanning Calorimeter (DSC-7, PerkinElmer, Inc., Waltham, MA, USA) was used to study the thermal characteristics of native starch, nano starch,

OSA starch, and OSA nano starch. The sample (3.5 mg) was weighed into an aluminum dish and distilled water was added. The dish was sealed and maintained at 25 °C for more than 12 h. The samples were heated from 10 to 200 °C at a heating rate of 10 °C/min. Using an empty aluminum plate as a reference, from the curve, the enthalpy of gelatinization (ΔH), the onset temperature (T_o), the peak temperature (T_p), and the end temperature (T_c) were obtained from data processing software provided by the differential scanning colorimetry (DSC) instrument.

Thermogravimetric analyses

Synchronous thermal analysis was carried out with thermogravimetric analyses (TGA; STA449C/4/G, Netsch, Selb, Germany). The starches used for thermal characterization were maintained at 33% relative humidity for over 24 h in advance. Samples weighing 3–6 mg were heated from 25 to 450 °C at a speed of 10 °C/min in a dynamic atmosphere of synthetic air with a flow rate of 100 mL/min. The sample weight of all samples was plotted as a function of temperature. Analysis was repeated twice for each sample.

Scanning electron microscopy

The morphologies of tiger nut native starch, OSA starch, nano starch and OSA nano starch were observed by using a scanning electron microscope (Zeiss Gemini 500, Carl Zeiss AG, Oberkochen, Germany) with voltage of 10 kV and current of PC 40. The starches were fixed on the specimen with conductive double-sided adhesive and sprayed with gold, and the sample was placed into the vacuum chamber for further observation. The samples were systematically observed at 1000× and 10 000× magnification.

Statistical analysis

The data were presented as means of the average of repeated measurements, and the results were given as mean±standard deviation (SD). One-way analysis of variance (ANOVA) was applied to check statistical significance with the least significant difference (LSD) test ($P<0.05$) by using SPSS 11.0 (SPSS Inc., Chicago, IL, USA). Image mapping was carried out using Origin 2018 (OriginLab, Northampton, MA, USA).

Results and Discussion

Effects of ultrasonication parameters on the starch particle size

As shown in Figure 2A, the starch concentration has a significant impact on nano starch preparation.It is clearly observed that the particle size of nano starch presents a bimodal distribution, and a starch concentration of 3% is the optimal starch concentration for preparing nano starch. The nano starch particles formed by a high concentration (4%–5%) of starch solution are large in size and uneven in size distribution. There may be two reasons for this; one is that the viscosity of the starch solution increases with increasing starch concentration. The starch solution with high viscosity has greater mass transfer resistance, which affects the diffusion speed between the starch solution and ethanol, increases the action time of polymer, and thus forms larger nanoparticles. Second, the higher the concentration of starch slurry, the more starch chains there are per unit volume. When the two phases are mixed, the starch chains natively carried by the polymer are more easily polymerized and wound with each other to form larger particles. The particle size distribution of nano starch prepared at different concentrations is shown in Figure 2B. It can be observed that a small amount of starch particles in the formed nano starch have a micron-sized peak with an approximate size of approximately 5–6 μm. When the ultrasonic time was 20 min, the ultrasonic power was 80%, and the slurry alcohol ratio was 1:2; with increasing starch concentration from 1% to 5%, the micron-sized peak grew, the peak with a peak value below 100 nm decreased, and the peak value increased from 52 to 71 nm. It can be assumed that, during ultrasonic treatment, a small amount of starch is not completely fragmented and the original structure of the starch remains, which leads to the existence of micron-sized starch particles in the final nano starch particles. In the nanoprecipitation process, the precipitated starch particles collide with the particles just entering the system or the precipitated particles aggregate to form larger particles, leading to an increase in the size of starch nanoparticles.

One of the mechanisms of ultrasonics is that the ultrasonic sound wave accelerates the collision and contact between solvent molecules and polymer molecules, which leads to cleavage of the C–C bond, and another mechanism is that the molecular chain is broken due to the cavitation effect of ultrasonic (Kumari *et al.*, 2020). During the preparation of nano starch by nanoprecipitation, ultrasonic cavitation effectively destroyed the internal structure of tiger nut starch molecules. Starch molecular chains contract and aggregate synchronously in ethanol solution, and precipitate out of the system under gravity to obtain nano starch particles with the smallest average particle size. After the ultrasonic treatment of starch paste, the size of tiger nut meal starch nanoparticles decreased significantly, because the ultrasonic treatment of starch solution can break the starch molecules, reducing the viscosity of the starch paste and improving the dispersion of starch molecules. As shown in Figure 2D, when the ultrasonic power is relatively low (60%–80%), the particle dimension of a few starch particles (size over 1 μm) in the final nano starch is larger due to incomplete ultrasonication. With increasing ultrasonic power, the mean particle size of the starch particles gradually decreases. There are basically no micron-sized starch particles in the prepared nano starch. However, when the ultrasonic power is too high (90%–100%), some starch molecules may aggregate again, leading to an increase in the particle size of starch nanoparticles. Therefore, as shown in Figure 2C, when the starch concentration was 2%, the ultrasonic time was 20 min, and the slurry alcohol ratio was 1:2, while the ultrasonic power was 80%, the size of the nano starch was the smallest.

Tiger nut starch molecules have a lamellar structure, and the ultrasonic wave causes the molecular surface to crack, and surface damage will increase with the ultrasonic time. It can be seen from Figure 2E that, with the continuous extension of ultrasonic treatment time, the starch particle size is roughly maintained in the range of 188–324 nm, and the PDI is also within the range of 0.4–0.5. When the treatment time was 10 min, the average particle size of starch nanoparticles was 188.48 nm (Table 1), and the distribution of starch nanoparticles was the most uniform at this time. At the same time, the concentration of starch solution was 2%, the ultrasonic power was kept at 80%, and the slurry alcohol ratio was set at 1:2. According to the research results of Yan *et al.* (2021), within 0–5 min, with the extension of ultrasonic time,

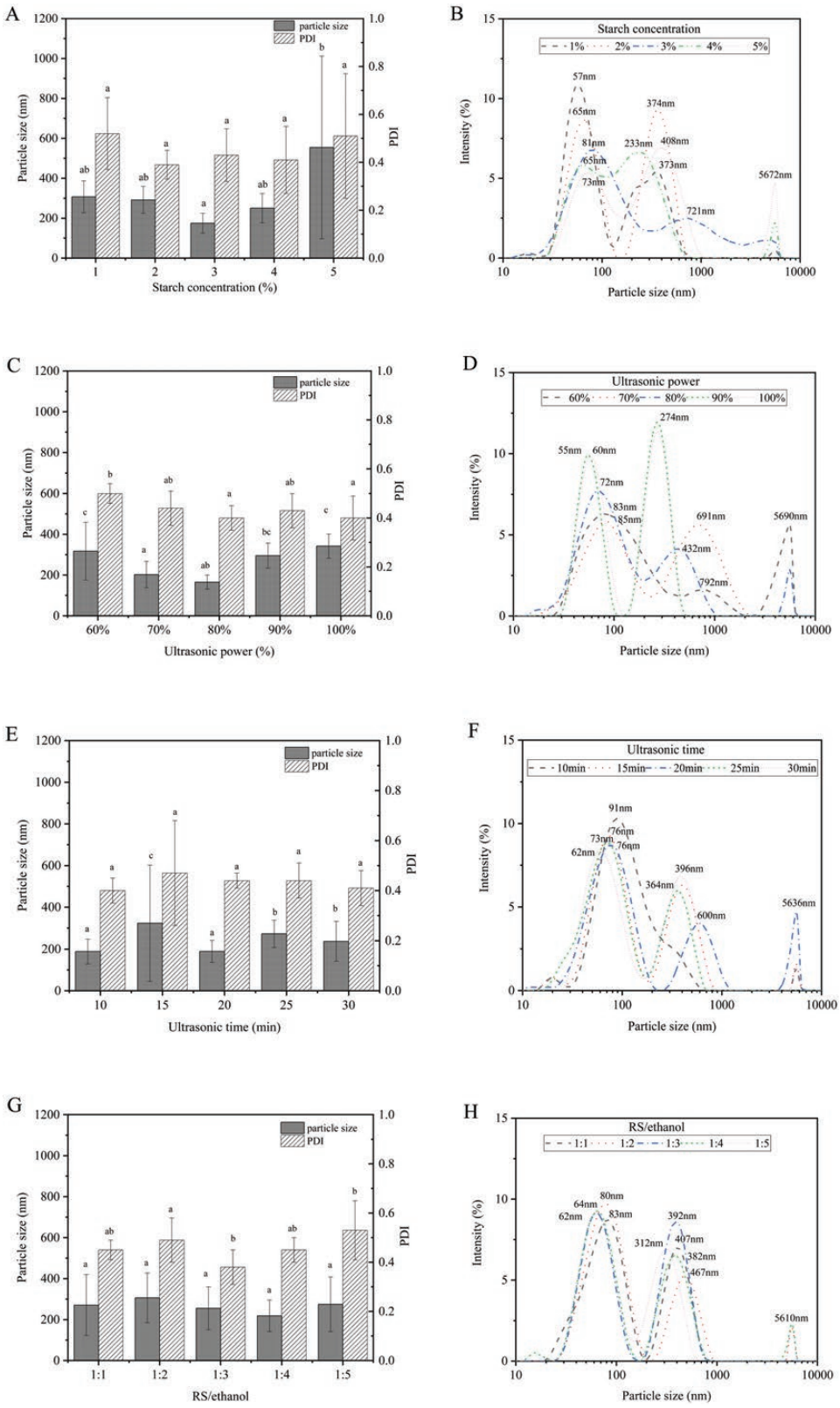

Figure 2. Particle size, polydispersity index (PDI), and size distribution of nano starch prepared with different parameters. Starch concentration (A–B); ultrasonic power (C–D); ultrasonic time (E–F); and volume ratios of starch solution to ethanol (G–H). Values are mean±standard deviation, and values with the same letters in the same column are not significantly different at $P<0.05$.

the particle size and dispersion index of starch nanoparticles gradually decrease, and there are significant differences. This research is in accordance with the result of this study. With increasing ultrasonic time, the particle size of the peak below 100 nm is smaller, and the particles with smaller particle size tend to aggregate, resulting in an increase in the middle peak.

Table 1. Mean particle size and polydispersity index (PDI) of nano starch prepared from different conditions before and after freeze-drying

Operation parameter		Before drying		After drying	
		Mean size (nm)	PDI	Mean size (nm)	PDI
Starch concentration	1%	307.34±79.29ab	0.52±0.15a	306.06±209.33a	0.43±0.09a
	2%	291.92±68.10ab	0.39±0.06a	298.60±123.92a	0.44±0.06a
	3%	174.58±49.57a	0.43±0.11a	280.88±75.94a	0.38±0.04a
	4%	250.24±73.63ab	0.41±0.14a	208.94±69.25a	0.43±0.09a
	5%	554.44±457.72b	0.51±0.26a	315.96±38.23a	0.40±0.03a
Ultrasonic time	10 min	188.48±59.68a	0.40±0.05a	183.46±33.89a	0.42±0.05a
	15 min	323.72±278.35a	0.47±0.21a	332.62±162.08a	0.50±0.12a
	20 min	188.98±52.69a	0.44±0.03a	242.92±67.76a	0.48±0.07a
	25 min	272.38±65.24a	0.44±0.07a	256.84±242.89a	0.55±0.11a
	30 min	237.34±95.04a	0.41±0.14a	195.02±37.72a	0.44±0.06a
Ultrasonic power	60% (360 W)	317.36±141.45c	0.50±0.04b	213.34±85.43a	0.43±0.04a
	70% (420 W)	202.34±64.40ab	0.44±0.07ab	281.30±160.61a	0.57±0.08b
	80% (480 W)	165.66±34.28a	0.40±0.05a	197.38±69.33a	0.45±0.08a
	90% (540 W)	295.04±61.47bc	0.43±0.07ab	201.48±40.62a	0.44±0.06a
	100% (600 W)	341.98±59.70c	0.40±0.09a	268.26±50.52a	0.46±0.07a
Slurry alcohol ratio	1:1	271.18±148.66a	0.45±0.04ab	327.34±142.59c	0.48±0.19a
	1:2	306.48±121.38a	0.49±0.09a	210.06±112.93ab	0.47±0.06a
	1:3	255.04±104.81a	0.38 ± 0.07b	321.54±106.00bc	0.93±0.06b
	1:4	218.62±76.75a	0.45 ± 0.05ab	169.84±42.70a	0.40±0.05a
	1:5	274.80±133.35a	0.53 ± 0.12b	243.72±51.29ab	0.46±0.07a

The total ultrasonic power was 600 W. Values are mean±standard deviation, and values with the same letters in the same column are not significantly different at $P<0.05$.

Instead, there will be continuous collision and polymerization of starch particles due to the extension of ultrasonic time, as shown in Figure 2F. Therefore, it is not the case that the longer the ultrasonic time is, the better the ultrasonic effect will be. On the one hand, the swelling and dissolution of starch nanoparticles caused by ultrasonic heating resulted in the release of a large number of amylose molecules, and increased the bonding sites of hydrogen bonds, which made it possible to embed different starch nanoparticles into the network of amylose molecules, thus forming larger starch particles (Dong *et al.*, 2021). On the other hand, it is possible that the bubble collapse caused by hollowing in the ultrasonic process leads to local overheating, which makes the Brownian motion of starch nanoparticles chaotic and accelerates the collision between particles. Small and medium particle aggregates will accumulate into larger aggregates, resulting in an increase in the final starch particles (Kumari *et al.*, 2020). In addition, hydrogen free radicals, hydroxyl free radicals, and sodium ions produced in the ultrasonic process may charge the nano starch particles, resulting in mutual attraction between starch particles and aggregation to shape large particles (Ruan *et al.*, 2022).

When preparing tiger nut meal starch nanoparticles, the starch slurry was added to the anhydrous alcohol solution in a dropwise manner. With the addition of starch slurry, the starch nanoparticles gradually deposit to form precipitation. The effect of the slurry alcohol ratio on the particle size of starch is similar to that of ultrasonic time (Figure 2G). The higher the ratio of slurry to ethanol, the smaller the particle size of nano starch; the result of this study is consistent with that of Chin *et al.* (2011), but the smaller nanoparticles are more likely to aggregate to form larger particles (Sadeghi *et al.*, 2017), which leads to the appearance of micron-sized peaks. When the amount of ethanol is small, there are always small starch granules that do not participate in the alcohol precipitation process. These starch granules would merge with precipitated starch grains, causing the formation of relatively large starch granules, as shown in Figure 2H.

Effect of drying on the particle size

It is apparent from inspection of Table 1 that the mean size and PDI of nano starches prepared under four different factors before and after freeze-drying were measured. When the water molecules enter the starch in the gelatinization process and cause the starch granules to expand, the water molecules are frozen in the starch during the freezing process, while the water sublimates during the freezing process, but the native structure and basic skeleton of the starch remain unchanged, which will lead to the particle size becoming larger. In this study, the particle size of most starch nanoparticles decreased after freeze-drying, which is different from other research results (Bel Haaj *et al.*, 2013; Dong *et al.*, 2022). This may be due to the difference in material composition, moisture content, moisture distribution, and moisture state of different materials. It may also be that in the processing of vacuum freeze-drying, the drying temperature is low and the dehydration is complete, making the surface of nano starch loose and porous, and the particle size after freeze-drying is smaller than that before freeze-drying (Chi *et al.*, 2020). Overall, considering the Z-average particle size and the PDI of nano starch before and after freeze-drying, the nano starch was prepared

for the following studies: when the starch concentration was 3%, the ultrasonic power was 80% of the total power as 480 W, the ultrasonic time was 10 min, and the slurry alcohol ratio was 1:4.

Physicochemical properties of native starch and nano starch

In the process of preparing nano starch, the structure of tiger nut native starch was destroyed, amylopectin was debranched, and the amylose content of nano starch (39.05%) increased by 15% compared with the native starch (24.10%). OSA esterification occurs mainly on the amylose chains, and the process of OSA modification introduces olefin chains into the starch, which results in longer amylose chains in the starch and further causes an increase in amylose content (Lopez-Silva *et al.*, 2019). It has also been suggested that the change in amylose content is attributed to OSA esterification or mild alkaline treatment during the modification process (Simsek *et al.*, 2015). There are also studies where nanoprecipitation does not change the amylose content of starch, with similar and different findings, which may be related to the type of starch (Dong *et al.*, 2022). The solubility and swelling power of the starch increased significantly, and the solubility and water retention property of the starch increased, as shown in Table S1. The solubility and swelling power of native starch and nano starch are significantly different. At 80 °C, the solubility of native starch is only 8.37%, while that of nano starch is 56.13%; the swelling power is similar to the solubility.

The solubility and swelling of native starch and nano starch at dissimilar temperatures are presented in Figure 3. The solubility and swelling degree can represent the water-holding capacity and internal binding capacity of tiger nut starch granules. The expansion and dissolution of starch are related to the proportion of amylose and amylopectin, molecular size, starch particle structure, the degree of combination between chains and the content of phospholipid compounds (Sánchez-Zapata *et al.*, 2012). As the amylose content of nano starch is higher than that of native starch, the solubility and expansion of nano starch are also relatively higher than those of native starch. The swelling of starch granule is generally attributed to amylopectin, which acts as a diluent and limits swelling (Akonor *et al.*, 2019). Figure 3A shows the solubility of native starch increases with increasing temperature. When the temperature reaches 75 °C, both the solubility and swelling power of nano starch increase the most. This may be because the double helix structure inside the starch disintegrates and begins to unwind when the temperature reaches approximately 80 °C.

Resistant starch contents

Table S2 shows the content of resistant starch in native starch, nano starch, OSA starch and OSA nano starch, which are 33.53%, 40.38%, 44.34%, and 37.76%, respectively. The resistant starch content in nano starch was higher than that in native starch, which is due to the strengthening of interaction between starch molecules and its perfect crystal structure (Yan *et al.*, 2022). Although the content of resistant starch in nano starch is higher than that in native starch, considering that the change range of content is not very significant this study wants to modify the starches, to study whether the modified starch can greatly increase the content of resistant starch. The OSA modification increases the content of amylose by introducing an alkenyl chain into starch, which leads to an increase in resistant starch content. OSA esterification occurs mainly on amylose chains, and the process of OSA modification introduces olefin chains into the starch, which results in longer amylose chains in the starch and further causes an increase in amylose content (Lopez-Silva *et al.*, 2019). It has also been suggested that the change in amylose content is attributed to OSA esterification or mild alkaline treatment during the modification process (Simsek *et al.*, 2015). Moreover, OSA starch has outstanding emulsification and embedding performance, good tolerance and stability to pH and other factors, and is positive for the structure change and function improvement of starch (Altuna *et al.*, 2018; Remanan and Zhu, 2023).

Thermal properties of starches

The thermal properties of starch are characterized in Figure 4 and Table S3. Native starch, nano starch, and OSA nano starch show different heat diagrams, so starch has different

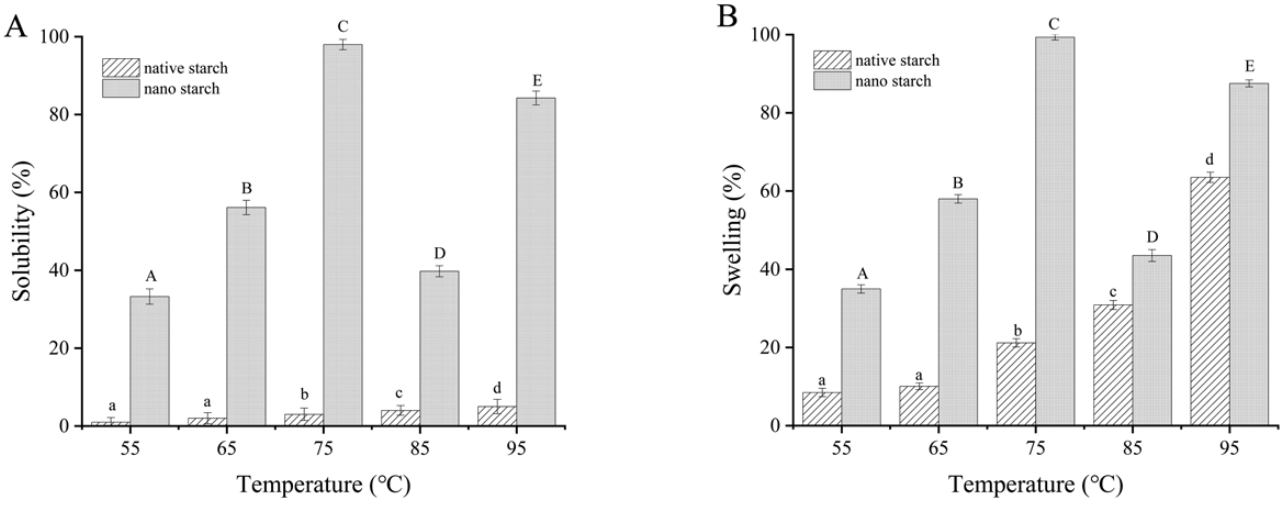

Figure 3. Solubility (A) and swelling (B) of native starch and nano starch. Values are mean±standard deviation, and values with the same letters in the same column are not significantly different at $P<0.05$.

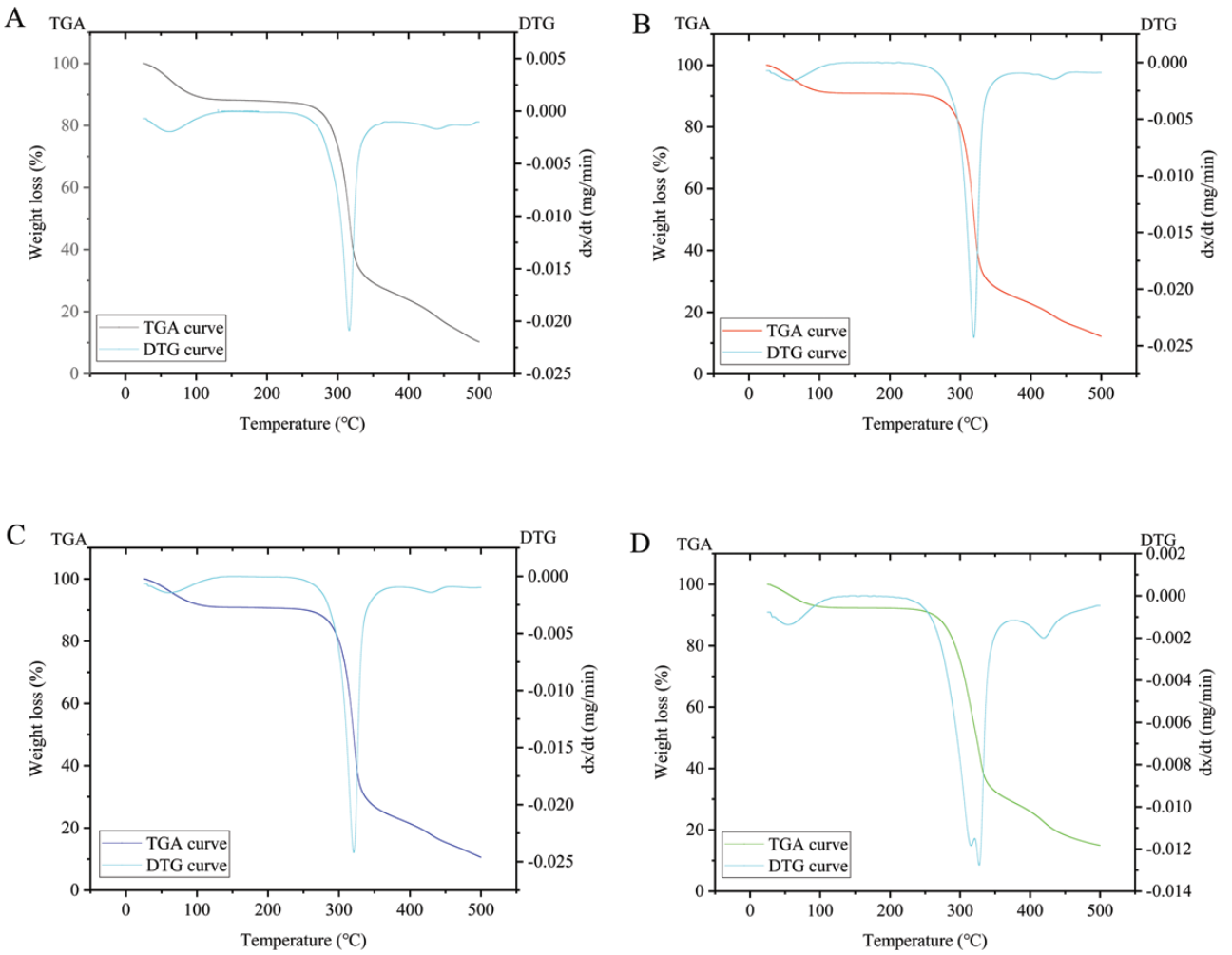

Figure 4. Thermogravimetric analyses (TGA) and DTG curves of native starch (A), nano starch (B), octenyl succinic anhydride (OSA) starch (C), and OSA nano starch (D).

heat properties. Wide endothermic peaks appeared at 55–164, 49–153, 48–141, and 52–170 °C in the gelatinization thermograms of native starch, nano starch, OSA starch, and OSA nano starch, respectively. In general, the melting peak onset temperature does not change much as the heating rate increases, while the peak top and peak end temperatures increase and the peak shape becomes wider. On the other hand, the sample may be incompletely dried or have impurities, and the peak will also widen (Khawas and Deka, 2016). The heat absorption peaks of both native starch and OSA starch were present in both physical mixtures, and the position of the peaks did not change except for the intensity change, indicating that the simple addition of OSA to native starch was only mechanical mixing without any additional covalent or non-covalent interaction between them. In contrast, the position of the heat absorption peak shifted in the thermal profile of the OSA–nano starch complex, indicating that the tiger nut nano starch and OSA combined to form an inclusion complex. Similar results have been found in studies by others (Cao *et al.*, 2023). After gelatinization and ultrasonic treatment, the structural integrity of tiger nut starch was destroyed. In the process of nano precipitation, the starch chain recrystallized to form a single spiral structure, and the thermal stability of recrystallized starch was reduced. Therefore, compared to native starch, nano starch began to gelatinize at a lower temperature, and a similar result was observed in previous research (Dong *et al.*, 2022). However, the structure of native starch is relatively firm, and the unwinding of double helix requires high energy to complete the phase transition, which has a high degradation temperature (Wu *et al.*, 2019). The thermal properties of tiger nut starches are mainly manifested by the difference between TGA and derivative thermogravimetry (DTG). As shown in Figure 4, the quality loss of native starch, nano starch and OSA starch has two main stages. The first stage is the loss of water in starch, and the second is the degradation of starch itself (Liang *et al.*, 2021). The decomposition of samples is mainly related to intermolecular forces, and the intermolecular hydrogen bond force is an important factor to ensure thermal stability. The introduction of hydrophobic groups may destroy the original sequence of starch particles, giving rise to the diminution of hydrogen bonds. Therefore, the intermolecular force of starch is weakened, the thermal stability of native starch and nano starch modified by OSA is weakened, and the initial gelatinization transition temperature T_0 of starch is lower than that of native starch, as illustrated in Table S3. The quality loss of OSA nano starch includes three stages, as shown in Figure 4D. The first mass loss occurred at 40.21–75.44 °C, the second at 292.87–335.52 °C, and the third at 412.26–438.45 °C. The first stage is related to the loss of water in starch, and the second is related to the degradation

of the starch itself. The weight loss in the temperature range of the third stage may be attributed to the formation of crystals and double helices with distinct stability after the starch sample was precipitated by nanoprecipitation and modified by OSA (Khawas and Deka, 2016).

The gelatinization transition temperatures (onset (T_0), peak (T_p), and conclusion (T_c)), temperature range (T_0–T_c), and enthalpy (ΔH) of native starch, nano starch, OSA starch, and OSA nano starch are presented in Table S3. The gel temperature of nano starch, OSA starch, and OSA nano starch is lower than that of native starch, which may be due to the introduction of an octenyl group in the polymer chain, which makes the particle structure unstable, leading to an increase in expansion volume and a decrease in gel temperature. The gelatinization temperature images the crystalline structure and degree of starch granules. Enthalpy of gelatinization formation (ΔH) stands for the energy required to separate the double-helix structure in the gelatinization process. The different crystallinity of starch is the reason for the temperature range of gelatinization. The heating temperature range of OSA nano starch is the highest, the heating temperature range of OSA starch is the lowest, and the gelatinization temperature range of native starch and nano starch is between OSA starch and OSA nano starch.

These results indicate that the OSA modification process increases the integrity of starch granules due to the interaction between the double helix in the crystal region of starch granules (Simsek *et al.*, 2012). Compared to native starch, nanoprecipitation leads to the enthalpy of gelatinization formation (ΔH). This may be due to the damage to the crystal structure during heating and ultrasound, the destruction of some double helices in the crystalline and amorphous regions of starch granules, and the significant reduction in the melting temperature and enthalpy of nano starch. Therefore, the energy entailed for separating the double-helix structure of nano starch granules is less (Dong *et al.*, 2022). This result is consistent with the previous report of Zhang *et al.* (2020). The modification weakens the interaction between starch molecules, leading to gelatinization at a lower temperature (Zhao *et al.*, 2021).

FT-IR analysis

The FT-IR analysis of four kinds of tiger nut starches is shown in Figure 5A. As we can see from Figure 5A, the wavenumber 3600–3200 cm^{-1} is the OH stretching vibration absorption peak of glucose unit, 2915 cm^{-1} is the asymmetric tensile vibration absorption peak of C–H, 1632 cm^{-1} is the absorption peak of water molecules in starch molecules, and 820–1280 cm^{-1} is mainly caused by highly interconnected C–O and C–C stretching vibration absorption peaks (Ahmad *et al.*, 2020). Compared with native starch, the movement of nanoparticles towards low wavenumber enables the hydrogen bond force between molecular chains in nanoparticles to become greater, and the structure among molecules becomes more inseparable (Yan *et al.*, 2022). Unlike microscale starches (native starch and OSA starch), nanoscale starches (nano starch and OSA nano starch) have characteristic peaks at 775 cm^{-1}, and a similar result was observed in another study, in which the result was attributed to the existence of β-glucosidic bond in the nano starches (Ahmad *et al.*, 2020).

Compared to native starch, the infrared spectrum of OSA starch showed new peaks 1724 cm^{-1} and 1572 cm^{-1}, indicating that the OSA group was successfully drawn into and integrated with native starch. The peak at 1724 cm^{-1} of starch has a bearing on stretching of –COOR, and another peak at 1572 cm^{-1} is related to the asymmetric tensile vibration of RCOO–. In addition, there is no obvious difference between the infrared spectra of different starches, indicating that no other substances are introduced into the starch after OSA modification (Chen *et al.*, 2014). This is consistent with the results reported by Liang and colleagues; after OSA modification, the structure of starch will change due to the addition of hydrophobic groups (Liang *et al.*, 2021).

XRD analysis

Figure 5B shows the XRD patterns of four kinds of tiger nut starches. Figure 5B shows that there are seven distinct characteristic peaks in the native starch of tiger nut meal, which are located at 15°, 16.9°, 17.8°, 20.8°, 23°, 26.5°, and 27.8°, and are typical A-type crystals (Yan *et al.*, 2021). Nano starch has weak single diffraction peaks at 19.7° and 26.5° and several

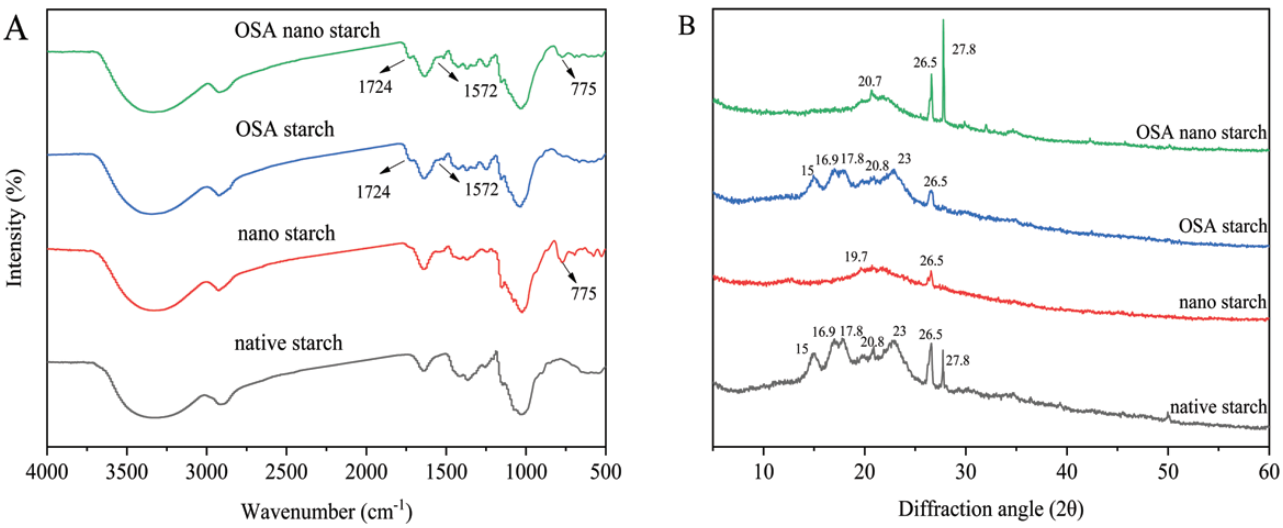

Figure 5. The Fourier transform infrared spectroscopy (FT-IR) (A) and X-ray diffraction patterns (B) of native starch, obtained starch nanoparticles, octenyl succinic anhydride (OSA) starch, and OSA nano starch.

characteristic peaks at approximately 15° have been flattened or even basically disappeared, indicating that the crystal structure of native starch has been destroyed. This may be due to gelatinization, and the hydrogen bonds within and between starch molecules are destroyed, which leads to the extension of the spiral structure area of starch and the destruction of the crystal structure of starch, resulting in the disappearance of diffraction peaks. On the other hand, ultrasonic cavitation produced by ultrasonic treatment will produce microbubbles in the solution. When bubbles break, high energy is transformed into high pressure and elevated temperature, leading to polymer degradation (Kumari *et al.*, 2020). Ultrasonic treatment destroyed the crystalline region of starch and decreased the crystallinity of nanoparticles. The crystallinity of nano starch was 5.76%, which was lower than that of native starch by 14.64%. The size of crystal, the length and content of amylopectin, the interaction of the double helix, and the orientation of the double-helix structure in the crystal all affect the difference in crystallinity. Native starch and nano starch have different amylopectin contents, different starch composition and properties, and different crystallinities.

The crystallinity of OSA starch is 19.01%, which is slightly superior to that of the native starch, which indicates that the modification mainly occurs in the non-oriented region, and has no obvious effect on the crystal structure of the starch itself, which is consistent with the results of electron microscope. OSA nano starch has a weak single diffraction peak at 20.7° and sharp diffraction peaks at 26.5° and 27.8°, suggesting the existence of plane structure with long arrangement structure. The crystallinity of OSA nano starch is 25.23%, which is significantly higher than that of nano starch. This indicates that ultrasonic treatment and nanoprecipitation are necessary on native starch prior to OSA modification. Ultrasonic treatment has an obvious effect on the starch structure and can help the substituents bind to the starch, thus changing the crystal structure of the starch.

Scanning electron microscopy analysis

The results are represented in Figure 6 and the influence of nano-precipitation on the morphological characteristics of the nano starch was obvious. A small amount of tiger nut starch is in the form of spherical granules, most of which are irregular flaky structures; and the spherical granules have threads on their surfaces. There are slight cracks on the surface of spherical starch particles due to drying (Figure 6B). The shape of nano starch is more uniform, most of them are spherical, the particle size is significantly smaller than tiger nut native starch, and the particle size of most starch nanoparticles is 100–500 nm. As a result of the desolvation in the drying process, there is a slight agglomeration between the particles. For starch samples, starch morphology may change significantly during storage, and amylose retrogradation will lead to reorganization of starch structure during storage.

Compared to native starch, the original irregular flake of OSA starch became more finely divided, and the overall shape did not change obviously. This may be because the reaction of native starch occurred only on the surface of the starch during the OSA modification. In addition, from Figures 6B and 6F, the size of spherical starch particles also changed at the same magnification, which indicated that the effect of direct OSA modification on tiger nut starch was poor. However, the surface of starch nanoparticles modified by OSA is smooth, and the shape is very regular oblate (Figure 6H). Compared with native starch, the morphology of OSA nano starch changes significantly. A mixture of slender fiber-like particles and oblate particles was observed in Figure 6G, indicating that the effect of OSA modification of tiger nut native starch is better and the structure of nano starch is easier to change. This may be because during the preparation of OSA nano starch, the anhydride bond of OSA is broken, one end forms an ester bond with the hydroxyl group on the starch molecule, and the other end forms carboxylic acid, which reacts with starch to form octenyl succinic acid starch ester containing hydrophilic and hydrophobic groups. The introduction of hydrophobic groups makes OSA starch amphiphilic, which affects the surface and internal order of starch particles, thus causing obvious changes in starch structure. The surface of OSA nano starch is smooth, and the shape is very regular oblate. Compared with native starch, the morphology of starch changes significantly, from the native lamellar structure to columnar and spherical (Quintero-Castano *et al.*, 2020).

The nano starch particles modified by OSA after drying show a slender fiber structure (Figure 6G) and an oblate shape (Figure 6H), and a similar phenomenon was observed in another study (Su *et al.*, 2022). In the process of OSA modification of nano starch, polymerized nanoparticle monomers were dissociated by OSA groups in the aqueous phase system. Due to the introduction of octenyl succinic anhydride, OSA nano starch particles reaggregated to form a micelle under the combined action of hydrogen bond and hydrophobic interaction. Hydrophilic groups, such as hydroxyl groups, in nano starches made them dissolve in water to form oblate starch particles with a hydrophilic surface and a hydrophobic interior. OSA groups adhere to the surface of nano starch, forming short fibers, which are extended to form longer fibers by the interaction of gelation and surfactant, and further form a fibrous network structure by the interaction of water-soluble supramolecular polymerization and surfactant-induced dilution, as shown in Figure 6G.

Conclusions

In conclusion, starch was successfully isolated from tiger nut meals and used to prepare starch nanoparticles by gelatinization, ultrasonication, and nanoprecipitation under different conditions. The optimized conditions for nano starch preparation were as follows: starch concentration of 3%, ultrasonic power of 80%, ultrasonic time of 10 min, and slurry alcohol ratio of 1:4. The prepared nano starch showed higher amylose content, solubility and swelling power than native starch. Through OSA modification, both native starch and nano starch obtained amphiphilic properties, which caused difference in the resistant starch content and thermal properties, indicating changes in digestion and gelatinization properties. FT-IR, XRD and scanning electron microscopy analysis confirmed the changes in microstructure. OSA-modified nano starch showed special structural characteristics, such as a slender fiber structure and a regular oblate structure. The hydrophobic OSA groups integrated on the nano starch aggregated to form hydrophobic cavities with hydrophilic surface in aqueous phase. This interesting finding inspires us to develop OSA nano starch as a carrier material in the nutraceutical, food, and pharmaceutical fields. Further research

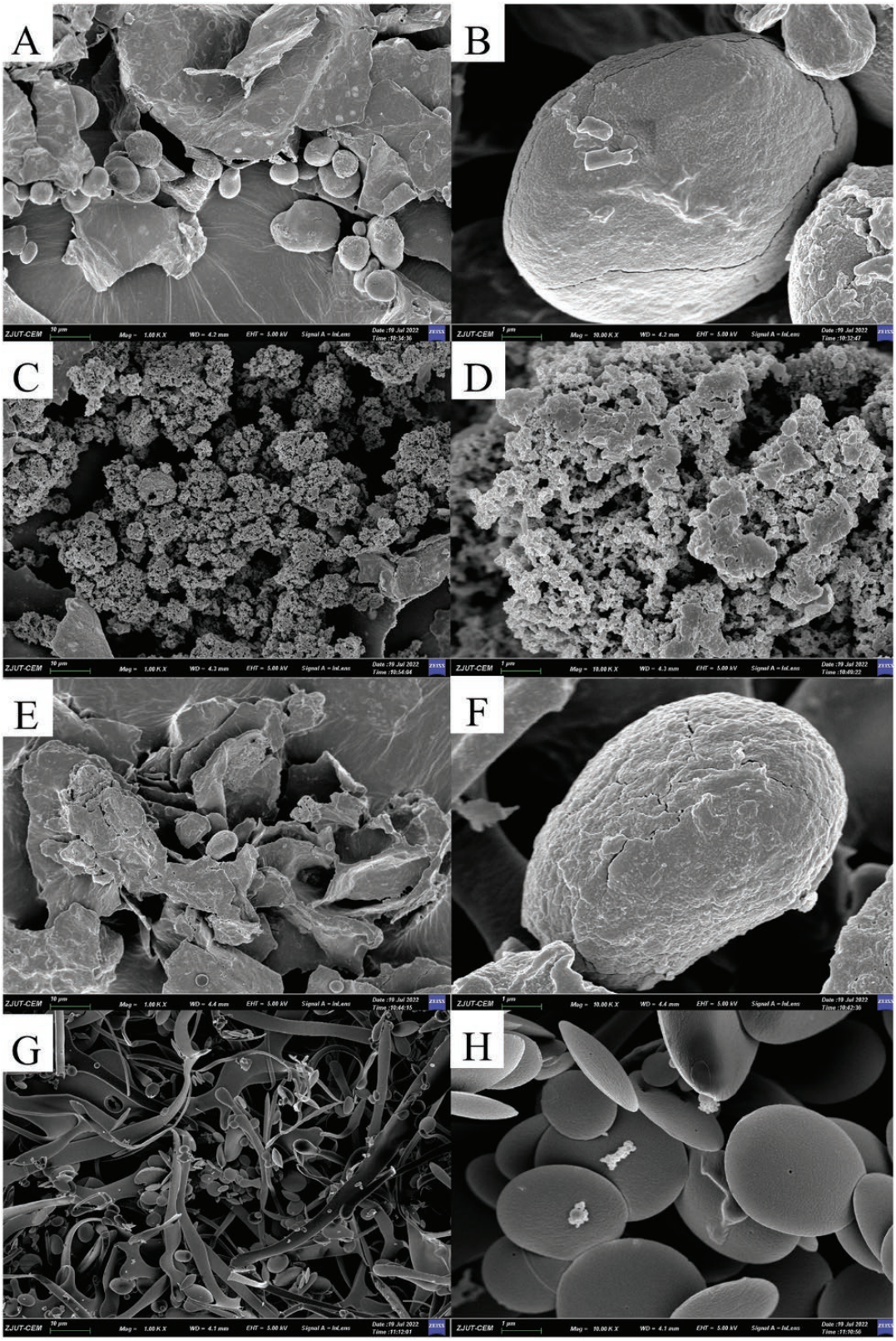

Figure 6. Scanning electron microscopy (SEM) micrographs of native starch (A: 1000×, B: 10 000×), nano starch (C: 1000×, D: 10 000×), OSA starch (E: 1000×, F: 10 000×), and octenyl succinic anhydride (OSA) nano starch (G: 1000×, H: 10 000×).

will focus on the potential applications of OSA nano starch as nanocapsules and emulsifying agents for the preparation of nanoemulsions.

Supplementary Material

Supplementary material is available at *Food Quality and Safety* online.

Acknowledgments

The authors would like to acknowledge Jilin Fuxiang Biotechnology Co., Ltd. for supplying the tiger nut meals.

Funding

This work was supported by the Key Research and Development Projects of Zhejiang (No. 2022C04021) and Zhejiang Provincial Natural Science Foundation (No. LQ23C200013), China.

Author Contributions

Wang Jian: Conceptualization, methodology, review & editing. Zhang Rui: Data curation, software, writing original draft. Huang Zhenyu: Visualization, investigation. Cai Ming: Supervision. Lou Wenyu: Validation. Wang Yan: Resources. Gharsallaoui Adem: Review & editing. Roubik Hynek: Review & editing. Yang Kai: Supervision, funding acquisition. Sun Peilong: Supervision, project administration.

Conflict of Interest

The authors declare that they do not have any commercial or associative interest that represents any conflict of interest in connection with this work.

References

Ahmad, M., Gani, A., Hassan, I., *et al.* (2020). Production and characterization of starch nanoparticles by mild alkali hydrolysis and ultra-sonication process. *Scientific Reports*, 10(1): 3533.

Akonor, P. T., Tortoe, C., Oduro-Yeboah, C., *et al.* (2019). Physicochemical, microstructural, and rheological characterization of tigernut (*Cyperus esculentus*) starch. *International Journal of Food Science*, 2019: 3830651.

Altuna, L., Herrera, M. L., Foresti, M. L. (2018). Synthesis and characterization of octenyl succinic anhydride modified starches for food applications. A review of recent literature. *Food Hydrocolloids*, 80: 97–110.

Bel Haaj, S., Magnin, A., Petrier, C., *et al.* (2013). Starch nanoparticles formation via high power ultrasonication. *Carbohydrate Polymers*, 92(2): 1625–1632.

Cao, F., Zheng, M., Wang, L., *et al.* (2023). Amylose and amylopection contents affect OSA-esterified corn starch's solubilizing efficacy and action mode on hesperetin. *LWT-Food Science and Technology*, 183: 114904

Chen, M., Yin, T., Chen, Y., *et al.* (2014). Preparation and characterization of octenyl succinic anhydride modified waxy rice starch by dry media milling. *Starch*, 66(11–12): 985–991.

Chi, C., Li, X., Zhang, Y., *et al.* (2020). Understanding the effect of freeze-drying on microstructures of starch hydrogels. *Food Hydrocolloids*, 101: 105509.

Chin, S. F., Pang, S. C., Tay, S. H. (2011). Size controlled synthesis of starch nanoparticles by a simple nanoprecipitation method. *Carbohydrate Polymers*, 86(4): 1817–1819.

Cortés, C., Esteve, M. J., Frígola, A., *et al.* (2005). Quality characteristics of horchata (a Spanish vegetable beverage) treated with pulsed electric fields during shelf-life. *Food Chemistry*, 91(2): 319–325.

Defelice, M. S. (2002). Yellow nutsedge *Cyperus esculentus* L.—snack food of the gods. *Weed Technology*, 16(4): 901–907.

Dong, H., Zhang, Q., Gao, J., *et al.* (2021). Comparison of morphology and rheology of starch nanoparticles prepared from pulse and cereal starches by rapid antisolvent nanoprecipitation. *Food Hydrocolloids*, 119: 106828.

Dong, H., Zhang, Q., Gao, J., *et al.* (2022). Preparation and characterization of nanoparticles from cereal and pulse starches by ultrasonic-assisted dissolution and rapid nanoprecipitation. *Food Hydrocolloids*, 122: 107081.

Ezeh, O., Gordon, M. H., Niranjan, K. (2014). Tiger nut oil (*Cyperus esculentus* L.): a review of its composition and physico-chemical properties. *European Journal of Lipid Science and Technology*, 116(7): 783–794.

Khawas, P., Deka, S. C. (2016). Effect of modified resistant starch of culinary banana on physicochemical, functional, morphological, diffraction, and thermal properties. *International Journal of Food Properties*, 20(1): 133–150.

Kumari, S., Yadav, B. S., Yadav, R. B. (2020). Synthesis and modification approaches for starch nanoparticles for their emerging food industrial applications: a review. *Food Research International*, 128: 108765.

Li, X., Fu, J., Wang, Y., *et al.* (2017). Preparation of low digestible and viscoelastic tigernut (*Cyperus esculentus*) starch by *Bacillus acidopullulyticus* pullulanase. *International Journal of Biological Macromolecules*, 102: 651–657.

Li, Y., Gao, Q. (2023). Novel self-assembly nano OSA starch micelles controlled by protonation in aqueous media. *Carbohydrate Polymers*, 299: 120146.

Liang, S., Hong, Y., Gu, Z., *et al.* (2021). Effect of debranching on the structure and digestibility of octenyl succinic anhydride starch nanoparticles. *Food Science and Technology*, 141: 111076.

Liu, X. X., Liu, H. M., Li, J., *et al.* (2019). Effects of various oil extraction methods on the structural and functional properties of starches isolated from tigernut (*Cyperus esculentus*) tuber meals. *Food Hydrocolloids*, 95: 262–272.

Liu, H. M., Yan, Y. Y., Liu, X. X., *et al.* (2020). Effects of various oil extraction methods on the gelatinization and retrogradation properties of starches isolated from tigernut (*Cyperus esculentus*) tuber meals. *International Journal of Biological Macromolecules*, 156: 144–152.

Lopez-Silva, M., Bello-Perez, L. A., Alvarez-Ramirez, J., *et al.* (2019). Effect of amylose content in morphological, functional and emulsification properties of OSA modified corn starch. *Food Hydrocolloids*, 97: 105212.

Pascual, B., Maroto, J. V., LóPez-Galarza, S., *et al.* (2000). Chufa (*Cyperus esculentus* L. var. sativus boeck.): an unconventional crop. Studies related to applications and cultivation. *Economic Botany*, 54(4): 439–448.

Quintero-Castano, V. D., Castellanos-Galeano, F. J., Alvarez-Barreto, C. I., *et al.* (2020). Starch from two unripe plantains and esterified with octenyl succinic anhydride (OSA): partial characterization. *Food Chemistry*, 315: 126241.

Remanan, M. K., Zhu, F. (2023). Encapsulation of rutin in Pickering emulsions stabilized using octenyl succinic anhydride (OSA) modified quinoa, maize, and potato starch nanoparticles. *Food Chemistry*, 405: 134790.

Ruan, S., Tang, J., Qin, Y., *et al.* (2022). Mechanical force-induced dispersion of starch nanoparticles and nanoemulsion: size control, dispersion behaviour, and emulsified stability. *Carbohydrate Polymers*, 275: 118711.

Sadeghi, R., Daniella, Z., Uzun, S., *et al.* (2017). Effects of starch composition and type of non-solvent on the formation of starch nanoparticles and improvement of curcumin stability in aqueous media. *Journal of Cereal Science*, 76: 122–130.

Sánchez-Zapata, E., Fernández-López, J., Angel Pérez-Alvarez, J. (2012). Tiger nut (*Cyperus esculentus*) commercialization: health aspects, composition, properties, and food applications. *Comprehensive Reviews in Food Science and Food Safety*, 11(4): 366–377.

Simsek, S., Ovando-Martinez, M., Whitney, K., *et al.* (2012). Effect of acetylation, oxidation and annealing on physicochemical properties of bean starch. *Food Chemistry*, 134(4): 1796–1803.

Simsek, S., Ovando-Martinez, M., Rayner, M., *et al.* (2015). Chemical composition, digestibility and emulsification properties of octenyl succinic esters of various starches. *Food Research International*, 75: 41–49.

Su, L., Mosquera, J., Mabesoone, M. F. J., *et al*. (2022). Dilution-induced gel–sol–gel–sol transitions by competitive supramolecular pathways in water. *Science*, 377(6602): 213–218.

Sun, Q. (2018). Starch nanoparticles. In: Woodhead Publishing Series in Food Science, Technology and Nutrition, Starch in Food (Second Edition). Woodhead Publishing, Cambridge, UK, pp. 691–745.

Sweedman, M. C., Tizzotti, M. J., Schafer, C., *et al*. (2013). Structure and physicochemical properties of octenyl succinic anhydride modified starches: a review. *Carbohydrate Polymers*, 92(1): 905–920.

Wang, J., Yu, Y. D., Zhang, Z. G., *et al*. (2022). Formation of sweet potato starch nanoparticles by ultrasonic-assisted nanoprecipitation: effect of cold plasma treatment. *Frontiers in Bioengineering and Biotechnology*, 10: 986033.

Wu, J., Huang, Y., Yao, R., *et al*. (2019). Preparation and characterization of starch nanoparticles from potato starch by combined solid-state acid-catalyzed hydrolysis and nanoprecipitation. *Starch*, 71(9–10): 1900095.

Yan, X., Diao, M., Yu, Y., *et al*. (2021). Influence of esterification and ultrasound treatment on formation and properties of starch nanoparticles and their impact as a filler on chitosan based films characteristics. *International Journal of Biological Macromolecules*, 179: 154–160.

Yan, X., Diao, M., Yu, Y., *et al*. (2022). Characterization of resistant starch nanoparticles prepared via debranching and nanoprecipitation. *Food Chemistry*, 369: 130824.

Ye, F., Miao, M., Jiang, B., *et al*. (2017a). Elucidation of stabilizing oil-in-water Pickering emulsion with different modified maize starch-based nanoparticles. *Food Chemistry*, 229: 152–158.

Ye, F., Miao, M., Lu, K., *et al*. (2017b). Structure and physicochemical properties for modified starch-based nanoparticle from different maize varieties. *Food Hydrocolloids*, 67: 37–44.

Yu, M., Ji, N., Wang, Y., *et al*. (2021). Starch-based nanoparticles: stimuli responsiveness, toxicity, and interactions with food components. *Comprehensive Reviews in Food Science and Food Safety*, 20(1): 1075–1100.

Zhang, Y., Dai, Y., Hou, H., *et al*. (2020). Ultrasound-assisted preparation of octenyl succinic anhydride modified starch and its influence mechanism on the quality. *Food Chemistry: X*, *5*: 100077.

Zhang, J., Ran, C., Jiang, X., *et al*. (2021). Impact of octenyl succinic anhydride (OSA) esterification on microstructure and physicochemical properties of sorghum starch. *Food Science and Technology*, 152: 112320.

Zhao, Y., Khalid, N., Nakajima, M. (2021). Fabrication and characterization of dodecenyl succinic anhydride modified kudzu starch. *Starch*, 74(1–2): 2100188.